

UDC 669.298.3:620.184

EFFECT OF THE GRAIN SIZE AND DEFORMATION SUBSTRUCTURE OF AUSTENITE ON THE CRYSTAL GEOMETRY OF BAINITE AND MARTENSITE IN LOW-CARBON STEELS

N. Yu. Zolotarevskii,¹ A. A. Zisman,² S. N. Panpurin,¹ Yu. F. Titovets,¹ S. A. Golosienko,² and E. I. Khlusova²

Translated from *Metallovedenie i Termicheskaya Obrabotka Metallov*, No. 10, pp. 39 – 48, October, 2013.

The effect of deformation in the austenitic temperature range on the features of the crystal geometry of the packet-and-block structure of martensite and bainite after cooling is studied for two low-carbon steels with different levels of microalloying. The distribution of lattice off-orientations in the substructure of the austenite formed by hot deformation of a model austenitic steel SS304 is determined. The effect of the grain size of the austenite and of the cooling rate on the bainite and martensite effective grain sizes is investigated. The results are analyzed.

Key words: steel, structure, orientation relation, austenite, bainite, martensite.

INTRODUCTION

The first studies of the crystal geometry of martensite laths were performed by Russian scientists in the 1970s [1, 2]. However, only the recent introduction of the panoramic EBSD-method based on scanning electron microscopy into the practical metals science has made it possible to perform detailed crystallographic analysis of complex multilevel structures due to the polymorphic transformation in steels. Specifically, this method has been used for determining important features of the structure of bainite as a function of the cooling rate [3] and for analyzing in detail the martensitic and bainitic structures after transformation under isothermal conditions [4, 5].

The structure of bainite in low-carbon steels has a primarily lath morphology and is similar in this respect to the structure of lath martensite. The laths representing crystals of α -phase with a thickness of at most 1 μm group in bainite and in lath martensite into larger structural components, i.e., packets and blocks [1 – 5]. The packets are regions discernible with the help of light microscopy, where the laths on the surface of a lap are arranged at about the same angle due to closeness of the habit planes. At the same time, the morphologically united packets consist of blocks with different crystallographic orientations. Today a block is understood [4] as

a region consisting of laths with about the same orientation of the crystal lattice, which is detectable as a whole entity by a standard EBSD analysis.

An important task in analyzing martensite and bainite structures, the solution of which has become possible upon the appearance of novel instrumentation, is singling out of “effective grains” separated by large-angle boundaries. Such crystal components, which can be represented by packets or individual blocks, determine the resistance of the material to crack propagation [6, 7]. At the same time, the distinctive features of the packet-and-block structure in bainitic and martensitic steels have not been studied exhaustively. It remains unclear how the geometric features of crystals in such structures depend on the mode of thermomechanical treatment.

It has been shown in [8 – 10] that hot deformation of the initial austenite causes growth of martensite packets. Similar effects have been determined in bainite too [10]. However, inheritance of the deformation substructure of austenite [11] and increase in the number of places of nucleation promote refinement of the transformed structure of the steel, which is often observed in steels with a structure of granular bainite [12]. Thus, the effect of deformation on the packet-and-block structure of martensite and bainite seems to be contradictory. The complexity of the problem is aggravated by inappropriate knowledge of the structure of the hot-deformed austenite itself. The situation has changed in this respect only recently, due to studies of model austenitic alloys with deformation properties close to those of the austenite of low-carbon steels

¹ St. Petersburg State Polytechnic University, St. Petersburg, Russia (e-mail: zolotarevsky@phmf.spbstu.ru).

² Central Research Institute of Structural Materials “Prometey” (CRISM “Prometey”), St. Petersburg, Russia.

TABLE 1. Chemical Composition of Studied Steels

Steel	Content of elements, wt.%					
	C	Mn	Si	Ni + Cu	Mo + Cr	V
1	0.08 – 0.10	0.2 – 0.3	0.5 – 0.6	2.2 – 2.9	0.5 – 1.0	0.04 – 0.06
2	0.08 – 0.10	0.3 – 0.4	0.3 – 0.4	5.0 – 5.5	1.0 – 1.5	0.10 – 0.20

that undergo a polymorphic transformation in cooling [13, 14].

The aim of the present work was to study the effect of modes of hot deformation on the substructure of austenite grains prior to polymorphic transformation in a model austenitic steel of grade SS304 and on the characteristics of the packet-and-block structure of martensite and bainite after cooling of two differently alloyed low-carbon steels from the austenitic range.

METHODS OF STUDY

The deformation structure of austenite was studied for steel SS304 that does not undergo $\gamma \rightarrow \alpha$ transformation during cooling and, as it has been shown earlier in [13, 14], is a suitable material for simulating the austenite of low-carbon steels.

We treated steel SS304 in two modes. Mode 1 involved heating at a rate of 10 K/sec to 1280°C, a hold for 300 sec, cooling at a rate of 40 K/sec to 1100°C, a hold for 5 sec, deformation to strain $\varepsilon = 15\%$, and a hold for 100 sec. Such a treatment yielded austenite with a mean grain size of about 90 μm . Then the specimens were cooled at a rate of 40 K/sec to 850°C, deformed to $\varepsilon = 30$ and 50% (the true strain was 0.35 and 0.7 respectively), and then quenched. To obtain larger austenite grains (about 190 μm) in mode 2 the specimens held at 1280°C for 300 sec were cooled immediately to 850°C, deformed to $\varepsilon = 50\%$, and then quenched.

The structure of bainite was studied for steel 1 (see Table 1). The metal was heat treated by heating at a rate of 5 K/sec to 1100 or 1200°C, held for 1 min, and cooled at a specified rate to room temperature. The mean size d_γ of the austenite grains uncovered by thermal etching in vacuum [15] was 47 and 140 μm after a hold at 1100 and 1200°C respectively. The tests on hot deformation of austenite were performed on cylindrical specimens 5 mm in diameter and 10 mm long with the help of a DIL-805 deformation dilatometer. The specimens were cooled at a rate of 5 K/sec from 1100 or 1200°C to 850°C; at 850°C they were deformed by compression by 30% at a rate of 1 sec^{-1} and quenched in an argon flow at a rate of 40 – 50 K/sec.

To study the structure of martensite we used a more alloyed steel 2 (see Table 1). The heat treatment involved heating at a rate of 40 K/sec to 1100°C, a hold of 100 sec ($d_\gamma \approx 80 \mu\text{m}$) or 300 sec ($d_\gamma \approx 160 \mu\text{m}$), cooling to 800°C at a rate of 40 K/sec, deformation by 30 or 50%, and cooling in

an atmosphere of argon at a rate of about 30 K/sec to room temperature.

The structure was studied by SEM with the help of a Quanta 3D FEG device at an accelerating voltage of 20 kV on conventional metallographic specimens subjected additionally to electrolytic polishing in an alcoholic solution of perchloric acid. Local orientations of the crystal lattice were scanned at a step of from 0.2 to 0.5 μm ; the EBSD were analyzed with the help of an automated Pegasus system of the EDAX Company.

The data obtained on the local orientations were used to estimate the crystal geometry of packet martensite and bainite on the basis of the orientation relation (OR) between the lattices of the γ - and α -phases. The orientation relation had been determined quite accurately earlier in [1] with the help of x-ray diffraction on single crystals with a structure of packet martensite. It differed from the Kurdjumov – Sachs ideal relation by the mean deviation of planes $(001)_\alpha$ from $(111)_\gamma$ by 0.4° and of directions $\langle 111 \rangle_\alpha$ from $\langle 011 \rangle_\gamma$ by 2.6°. The recent works performed with the help of EBSD have given close results [8, 9]. It has also been shown in [5] that a similar OR is obeyed in bainite of low-carbon steels.

In the present study of the bainite-martensite structures were studied in terms of the OR described in [8]. One crystal of a γ -phase (for example, one initial grain of austenite) may give rise to crystals of an α -phase with 24 different variants of orientation (we will use in what follows the recently accepted system for denoting these variants $V1 - V24$). Accordingly, every bainite or martensite block has an orientation matching one of these variants. Among the 24 variants we single out four groups ($V1 - V6$, $V7 - V12$, $V13 - V18$, and $V19 - V24$) in each of which any plane of type $\{110\}_\alpha$ is parallel to one of four planes of type $\{111\}_\gamma$.³ The scheme in Fig. 1a allows us to understand how six differing variants of orientation of the α -phase matching the Kurdjumov – Sachs OR may appear inside one group (inside one packet). It is common practice to describe the off-orientations between them for pairs $V1/V2$ (the off-orientation angle is about 60.2°), $V1/V3$ (about 59.6°), $V1/V4$ (about 5.4°), $V1/V5$ (about 59.6°), and $V1/V6$ (about 54.8°).⁴ The spectrum of the off-orientations between all the 24 variants formed from one grain of austenite is presented in Fig. 1b. It should be noted

³ Parallelism is obeyed only in the case of the Kurdjumov – Sachs orientation relation (OR), but with some deviation in experimental studies.

⁴ We give the values of the angles of off-orientation between the variants computed for the experimentally observed OR.

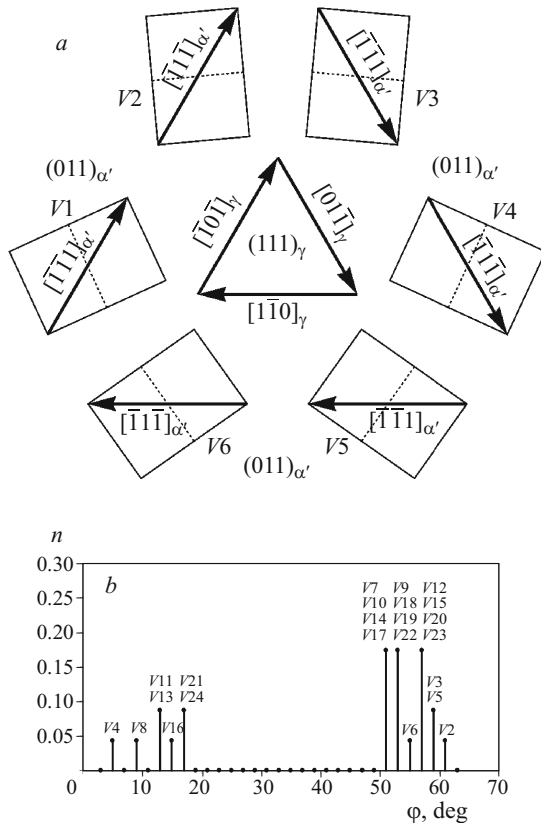


Fig. 1. Scheme of variants of implementation of interphase orientation relation (OR) inside one packet (*a*) and spectrum of crystallographic off-orientations in the α -phase between an arbitrarily chosen first variant V_1 and the rest of the variants (V_i) plotted under the assumption of their equiprobable appearance in the initial crystal of the γ -phase (*b*).

that these off-orientations include the off-orientations mentioned above between blocks belonging to one and the same packet and the off-orientations between blocks of different packets. The frequency and mutual arrangement of the formed blocks with orientations matching these variants determine finally the structure and properties of the steel [5, 9]. No wonder that the “problem of the choice of variants” attracts the attention of many researchers. We will term the boundaries with such off-orientations “crystallographically specified boundaries (CSB)” as it has been suggested in [16].

Other techniques for uniting variants of orientation of γ -phase are possible in addition to uniting a group on the basis of parallelism of close-packed planes of the α -phase. For example, they may be grouped on the basis of three possible variants of orientation of the Bain axis (the axis of compression in deformation of the lattice of the γ -phase that transforms it into a lattice of a α -phase) [4]. The off-orientations between the variants with parallel Bain axes give a subset of relatively low-angle CSB (below 20°) (Fig. 1). Dominating formation of groups of variants with parallel Bain axes has been determined, for example, in the structure of bainite of low-carbon steels [6, 5].

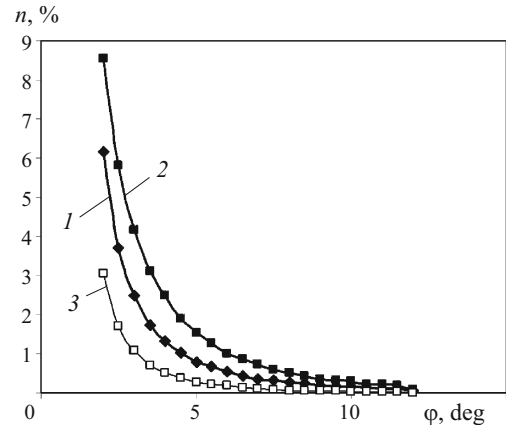


Fig. 2. Distribution of the off-orientations of the low-angle part of spectrum in steel SS304 after hot compressive deformation (n is the relative length of the corresponding boundaries with respect to the total length of the boundaries with angles $0.5^\circ < \varphi < 12^\circ$): 1) size of initial austenite grains $d_\gamma = 90 \mu\text{m}$, strain $\varepsilon = 30\%$; 2) $d_\gamma = 90 \mu\text{m}$, $\varepsilon = 50\%$; 3) $d_\gamma = 190 \mu\text{m}$, $\varepsilon = 50\%$.

Several works have appeared recently on the effect of deformation of austenite on the choice of variants in bainitic and martensitic transformations. It has been shown that the deformation reduces the number of implementable variants promoting the arrangement of the habit plane in parallel to the active slip planes [9]; this reduction results in growth in the mean size of packets.

RESULTS AND DISCUSSION

Deformation Substructure of Austenite

The distributions of intragrain off-orientations of austenite obtained by the EBSD method and presented in Fig. 2 agree with the earlier determined laws of the influence of deformation on the substructure of a model austenitic alloy 30% Fe – 70% Ni [14]. At the same time, the dependence of the deformation substructure on the grain size turned out to be unexpectedly strong. For example, for $\varepsilon = 50\%$ at a relatively small ($90 \mu\text{m}$) grain size the fraction of sub-boundaries with orientation angles exceeding 2° was about 35% of the total amount, whereas the growth of the grains by about a factor of 2 decreased this fraction by a factor of 5, and it did not exceed 9%. The more intense fragmentation of small grains may be explained by the fact that the process started on interfaces [17], though after the deformation with $\varepsilon = 50\%$ the corresponding structural inhomogeneity was discernible poorly (Fig. 3).

On the map of boundaries (Fig. 3*a*) obtained by EBSD-mapping of the structure of austenite after deformation with $\varepsilon = 50\%$, the boundaries with off-orientations matching various ranges of θ are depicted by gray and black lines. The corresponding mapping for $\varepsilon = 30\%$ is similar and we do not present it in this paper. The off-orientation angles on most sub-boundaries are $1 - 2^\circ$, i.e., are at a level exceed-

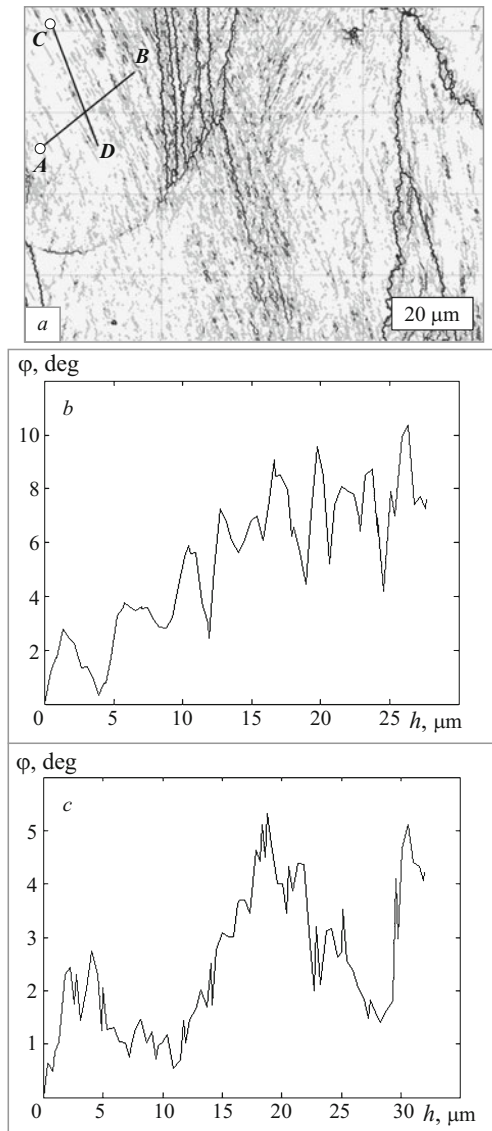


Fig. 3. Map of boundaries (*a*) and profiles of distribution of off-orientation φ with respect to the initial points *A* and *C* over segments *AB* (*b*) and *CD* (*c*) in steel SS304 ($d_\gamma = 90 \mu\text{m}$, $\varepsilon = 50\%$): the light-gray, dark-gray and black lines denote the boundaries with off-orientations $2^\circ < \varphi < 5^\circ$, $5^\circ < \varphi < 12^\circ$, and $\varphi > 12^\circ$ respectively.

ing inconsiderably the accuracy of a standard EBSD-analysis. At the same time, we should note that the kind of the substructure agrees with the results of a detailed study [13], in which low off-orientations were determined with the help of special filtering of the experimental data. It was shown that steel 304 under like deformation conditions acquired bands of subgrains with a mean size of about $1 \mu\text{m}$ and a mean off-orientation of about 1.5° .

On the map of a typical region of the structure of austenitic steel (Fig. 3*a*) the overwhelming majority of the sub-boundaries correspond to angle $\theta = 2 - 5^\circ$ (the light-gray lines), and the boundaries of an off-orientation exceeding 12° (the black lines) are primarily boundaries of initial grains and

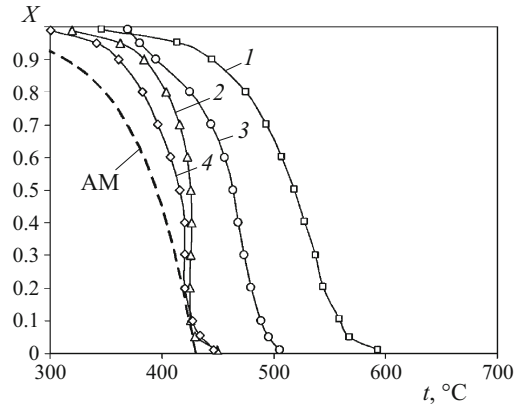


Fig. 4. Curves of decomposition of austenite (*X* is the volume fraction of the forming phase, *t* is the temperature) in steel *I* in the process of continuous cooling: 1) size of initial austenite grains $d_\gamma = 47 \mu\text{m}$, cooling rate $v_{\text{cool}} = 5 \text{ K/sec}$; 2) $d_\gamma = 47 \mu\text{m}$, $v_{\text{cool}} = 50 \text{ K/sec}$; 3) $d_\gamma = 47 \mu\text{m}$, strain $\varepsilon = 305$, $v_{\text{cool}} = 50 \text{ K/sec}$; 4) $d_\gamma = 140 \mu\text{m}$, $\varepsilon = 30\%$, $v_{\text{cool}} = 50 \text{ K/sec}$; AM) curve of formation of athermal martensite an accordance with the equation of Koistinen – Marburger.

twins. The grain boundaries exhibit individual regions strongly off-oriented relative to the surrounding substructure and possibly produced by dynamic recrystallization, but their contribution into the forming structure is very low. It can be seen that the substructure has about similar characteristics both near the grain boundaries and far from them. A similar picture is observed on other studied regions, i.e., the morphology and the level of the off-orientation may vary substantially from grain to grain, but within one grain the substructure is rather homogeneous.

Let us consider the characteristic profiles of the variation of the orientation over segments *AB* and *CD*, the first of which is located across subgrain bands and the second is inclined somewhat to the direction of the bands and intersects only three or four of them (Fig. 3*b* and *c*). It can be seen that the off-orientation upon intersection with extended band boundaries is on the whole higher than on the transverse sub-boundaries inside the band. At the same time, in both cases we observe substantial inhomogeneity of the orientation inside subgrains. Thus, the deformation structure is characterized by relatively low off-orientations on the boundaries separating subgrains at considerable gradients of the continuously varying orientation.

Bainite Structure

We studied the structure of steel *I* after heating to an austenitic condition, deformation (and without deformation), and subsequent cooling at various rates. The kinetics of the transformation in steel *I* for some cooling modes is presented in Fig. 4. With allowance for the presented kinetic curves, the possible components of the structure are bainite and martensite, because at a temperature below 600°C polygonal ferrite does not form in steels with composition studied.

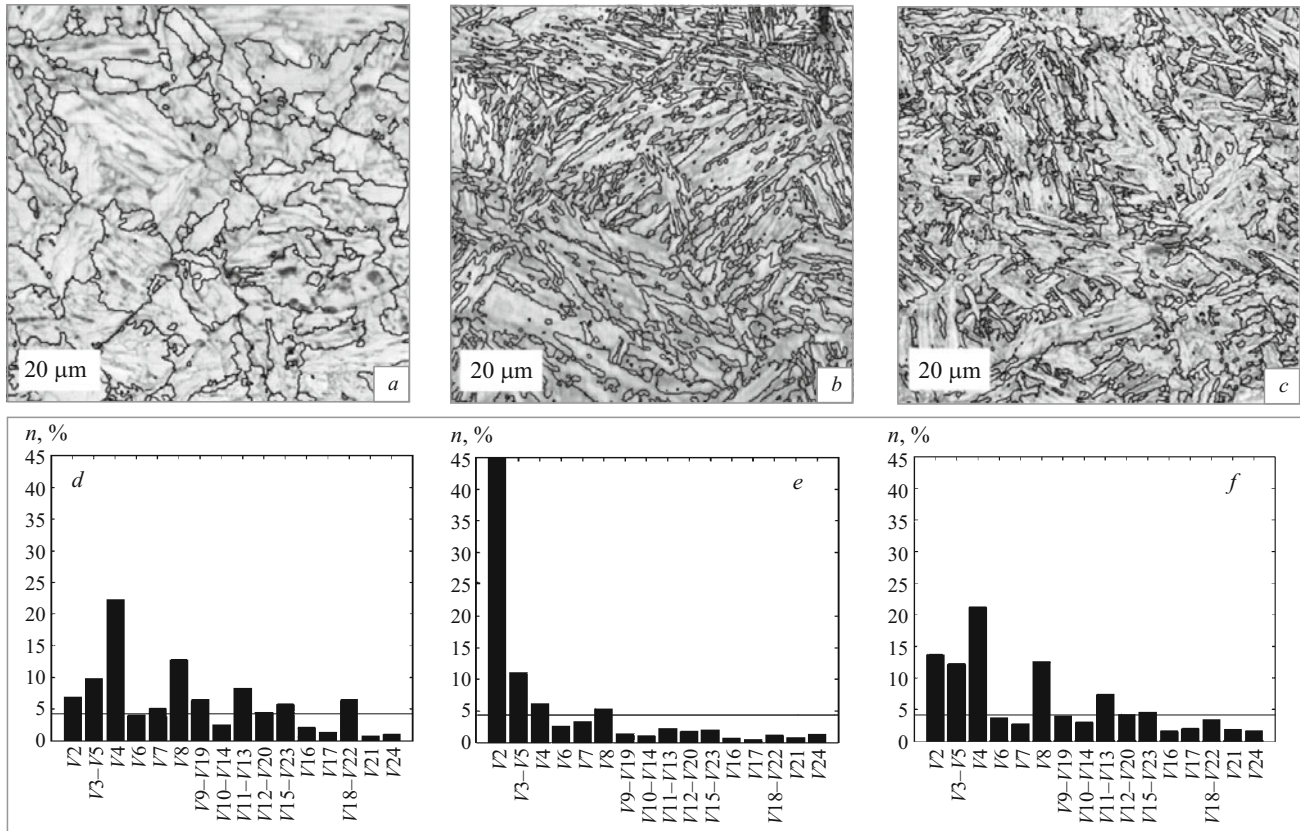


Fig. 5. Structure of steel *I* with mean size of initial austenite grains $d_\gamma = 47 \mu\text{m}$ presented as a map of distribution of parameter IQ characterizing the quality of the EBSD-image, onto which the contours of the boundaries (the black lines) with off-orientation exceeding 40° are superimposed (a – c), and relative lengths n of crystallographically specified boundaries (CSB) (d – f): a, d) cooling from the austenitic range (without deformation) at a rate $v_{\text{cool}} = 5 \text{ K/sec}$; b, e) $v_{\text{cool}} = 50 \text{ K/sec}$; c, f) deformation in the austenitic range with strain $\varepsilon = 30\%$, cooling with $v_{\text{cool}} = 50 \text{ K/sec}$.

The temperature of the start of martensitic transformation M_s for steel *I* is close to 430°C . Consequently, judging by the kinetic curves, the structure is represented by almost 100% ferrite at a low rate of cooling. In the case of cooling at a high rate, the transformation begins at about 450°C . At 430°C heat is emitted intensely, as a result of which the temperature remains constant at about 420°C for 4 sec, when a major part of the volume undergoes phase transformation. In this stage the bainitic reaction may be accelerated at the moment of the start of martensitic transformation [18]. At the same time, the proportion of athermal martensite (AM) cannot be high at this low supercooling below M_s , which is confirmed by the curve describing the dependence of the fraction of AM on the temperature T computed by the Koistinen – Marburger equation $\text{AM} = 1 - \exp(-\alpha(M_s - T))$ at $\alpha = 0.02 \text{ K}^{-1}$. Thus, bainite should dominate in the structure at a high cooling rate too.

In cooling of not deformed steel the grain size of the austenite affects little the kinetics of the bainitic transformation; the curves $X(T)$ for $d_\gamma = 140 \mu\text{m}$ at cooling rates of 5 and 50 K/sec virtually do not differ from the corresponding curves for $d_\gamma = 47 \mu\text{m}$. At the same time, the size of the aus-

tenite grains affects strongly the degree of influence of the preceding deformation of the austenite. For example, at $d_\gamma = 140 \mu\text{m}$ deformation with strain $\varepsilon = 30\%$ does not change the kinetics of the bainitic transformation, but at $d_\gamma = 47 \mu\text{m}$ (Fig. 4) the same deformation increases the temperature of the start of the transformation by about 50°C . The absence of such an effect for the case of larger austenite grains seems to be caused by their slower fragmentation.

Let us consider the factors determining the size of effective bainite grains separated by large-angle boundaries (we take into account the boundaries with off-orientation angles $> 40^\circ$, which are effective barriers for propagation of cleavage cracks [3]). Figure 5a – c present the structure of steel *I* with $d_\gamma = 47 \mu\text{m}$; Figure 5d – f present the relative fractions of CSB⁵ obtained under different conditions, which reflect

⁵ When we determined these spectra, the boundary was assumed to be close to the CSB if the deviation of the off-orientation on it from the ideal one between variants V1 – V24 did not exceed 1° . This low permissible deviation was chosen in order to avoid getting of some off-orientations into the interval of closeness to more than one CSB, among which their exist off-orientations rather close with respect to the angle and to the axis.

the obvious effect of the rate of cooling on the transformation. In slow cooling ($v_{\text{cool}} = 5$ K/sec) bainite has a granular morphology (Fig. 5a); in fast cooling the morphology is a lath one (Fig. 5b). In addition, the cooling rate affects considerably the choice of the variants of the OR. For example, at $v_{\text{cool}} = 5$ K/sec low-angle boundaries $V1/V4$ dominate inside packets, while the most frequent boundaries separating the blocks belonging to different packets are also $V1/V8$ and $V1/V11 + V13$, the off-orientations of which (9° and 12.5° respectively) move them closer to low-angle ones (Fig. 5d). Thus, the comparatively large size of the effective grains (in our case $9.3 \mu\text{m}$) is a result of the fact that the blocks inside packets are not strongly off-oriented, because the packets themselves are separated primarily by low-angle CSB. In the case of slow cooling ($v_{\text{cool}} = 50$ K/sec, Fig. 5b and e) the structure is organized oppositely. Then the dominant boundaries are intrapacket large-angle CSB $V1/V2$ and $V1/V3 + V5$. Therefore, though the packets in fast cooling are larger than in slow cooling, the effective grains are approximately three times smaller.

Small effective bainite grains also form in the case of preceding deformation of the steel with $d_\gamma = 47 \mu\text{m}$ in the austenitic temperature range after cooling at a rate of 50°C . However, their mean size ($3.8 \mu\text{m}$) is somewhat larger than without hot deformation ($3.2 \mu\text{m}$). Thus, the choice of variants after the deformation (Fig. 5f) becomes closer to the choice of variants without deformation at a lower cooling rate (Fig. 5d), and we should note that the deformation raises the temperature range of the transformation. In addition, the spectra for the low and high cooling rates (Fig. 5d and e) are similar to those obtained in [5] for high- and low-temperature holds in the bainitic temperature range. It is natural to assume that the special choice of variants of OR in deformed austenite is connected with the effect of the deformation on the temperature at which bainite forms.

Let us discuss briefly the mechanism of the choice of variants. In a shear transformation the formation of a crystal of an α -phase is accompanied by growth of internal stresses. A possible method for minimizing the elastic energy of the system is such a spatial organization of the arrangement of crystals in which the displacements produced by them are mutually compensated. This phenomenon is commonly termed self-accommodation [3–5]. It has been shown earlier in [1, 2] that self-accommodation in martensite occurs within every packet so that the total displacement inside the packet tends to zero. It seems that a similar mechanism of minimization of elastic energy develops in the lower part of the bainitic temperature range. A result of such a choice is dominance of large-angle boundaries separating blocks belonging to the same packet. When the temperature of the transformation increases, the accommodation mechanism seems to change. A suggestion has been put forward [3, 5] that austenite becomes more plastic upon growth in the temperature, and the role of plastic accommodation of austenite as a mechanism of minimization of the elastic energy in-

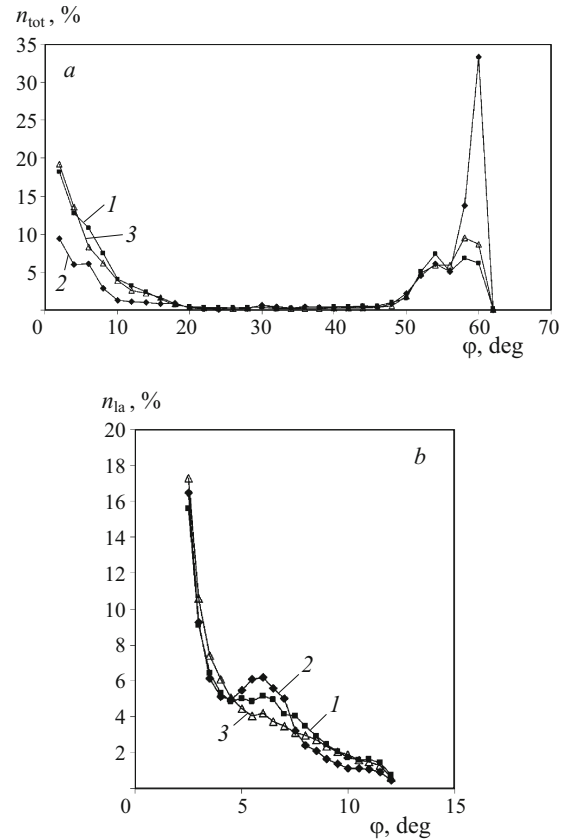


Fig. 6. Distribution of off-orientations in steel I with austenite grain size $d_\gamma = 47 \mu\text{m}$: a) total distribution (n_{tot} is the fraction of boundaries for the histogram with step 2°); b) low-angle part of the distribution (n_{la} is the fraction of boundaries for the histogram with step 0.5° in the number of boundaries in the range $2^\circ < \phi < 12^\circ$); 1, 2) cooling at a rate $v_{\text{cool}} = 5$ and 50 K/sec, respectively, without deformation in the austenitic range; 3) deformation with strain $\varepsilon = 30\%$, cooling with $v_{\text{cool}} = 50$ K/sec.

creases accordingly. By the data of [3] this may stimulate the formation of blocks with a common Bain axis forming relatively low-angle CSB between each other,

The distribution of off-orientations in a bainitic structure (Fig. 6a) changes depending on the treatment mode and in accordance with the change in the choice of variants described above. Let us consider the case of deformation of austenite, when the spectrum of the off-orientations in its low-angle part becomes close to that obtained without preceding deformation at a low cooling rate. In the earlier work [19] such an intensification of the low-angle peak was associated with the contribution of the off-orientations inherited from the plastically deformed austenite. However, the results of the present study (specifically, the kind of the distribution of the off-orientations in the substructure of the austenite) show that this effect is most probably caused by a change in the kind of the choice of variants toward a higher-temperature one, where the role of self-accommodation of structural transformations lowers due to the relatively high plasticity of

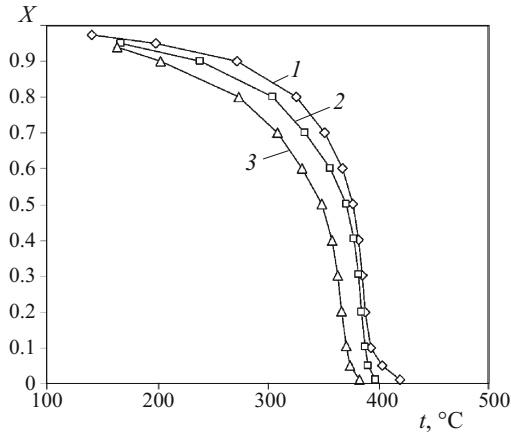


Fig. 7. Curves of decomposition of austenite (X is the volume fraction of the forming phase, t is the temperature) in steel 2 with $d_\gamma = 80 \mu\text{m}$: 1) after cooling at a rate 30 K/sec without deformation in the austenitic region; 2, 3) with deformation with strain $\varepsilon = 30\%$ and 50% respectively.

the austenite. This also explains the mentioned inconsiderable coarsening of the effective grains corresponding to structural components with off-orientation exceeding 40° . However, on the whole and with allowance for the growth in the total number of centers of nucleation of α -phase and in the content of boundaries with off-orientations ranging within $\theta = 2 - 20^\circ$, the preliminary deformation of the austenite causes refinement of the structure of bainite.

The low-angle part of the spectrum in angle range $2^\circ < \theta < 12^\circ$ is presented in detail in Fig. 6b. The low-angle boundaries $V1/V4$ (about 5.4°), $V1/V8$ (about 9°) and $V1/V11 + V13$ (about 12°)⁶ can contribute into this range. Individual laths that constitute blocks are also off-oriented in their turn by angles of several degrees [3, 4]. Overlapping, the distributions of the off-orientations between blocks and individual laths give the observed spectrum. It can be seen in Fig. 6b that without deformation in the austenitic domain ($\varepsilon = 0$) the spectrum contains a maximum that corresponds to off-orientation $V1/V4$. At $\varepsilon \neq 0$ the maximum is smeared, but on the whole the kind of the distribution is preserved. Thus, the deformation of the austenite only perturbs the spectrum typical for the substructure of bainite without changing it substantially. This agrees with the mentioned data on the level and kind of the distribution of off-orientations in deformed austenite.

Structure of Martensite

The dilatometric studies of the process of cooling of steel 2 at a rate of 30 K/sec after deformation in the austenitic

range (Fig. 7) show that the martensitic transformation in it prevails. The martensitic transformation starts at $M_s \cong 400^\circ\text{C}$. The presence of a low amount of bainite can be expected only in the case of $\varepsilon = 0$. It also follows from the data presented that the deformation of the austenite lowers somewhat the point M_s . At the same time, the change in the mean size of the austenite grains from 80 to $160 \mu\text{m}$ virtually does not influence the kinetics of the transformation in the steel studied.

The electron microscope studies of the steel with $d_\gamma = 160 \mu\text{m}$ show that the deformation with strain $\varepsilon = 50\%$ causes some refinement of the effective grains separated by large-angle boundaries (Fig. 8a and b). Measurements confirm this visual estimate; as a result of the deformation of the initial austenite the average size d_α decreases from 7 to $6 \mu\text{m}$. The tests at smaller austenite grains ($d_\gamma = 80 \mu\text{m}$) have given similar results. Thus, the size of the initial austenite grains and the preliminary deformation of the steel in the austenitic condition affect little the size of the effective grains in the martensitic structure.

Note that determination of effective grains is a quite conventional operation for a martensitic structure, because large-angle boundaries decelerate efficiently the propagation of a crack if the grains with such boundaries take a considerable part of the volume. However, this is not always valid for martensite. The fact is illustrated by Fig. 8, where very small isolated regions bounded by black contours can be seen against the background of a relatively weakly off-oriented structure. Thus, the concept of effective grains for a martensitic structure requires amendment.

The spectra of CSB (Fig. 8c and d), which are virtually independent of the deformation of the austenite, reflect important features of the martensitic structures of the steel studied. For example, at a relatively large size of packets ($40 - 60 \mu\text{m}$ for $d_\gamma = 160 \mu\text{m}$) formed by approximately parallel laths each packet contains a great number of blocks. A considerable part of the boundaries separating such blocks ($V1/V2$, $V1/V3 + V5$, $V1/V6$) are large-angle ones, while the fraction of the boundaries separating the blocks belonging to different packets is inconsiderable. The probable variant for the boundaries separating adjacent packets is $V1/V8$, and these boundaries are not large-angle ($\theta = 9^\circ$). Note that the spectra presented above agree well with the results of study [9] of the structure of martensite in another low-carbon steel, which proves the weak influence of the chemical composition and of the temperature M_s on the packet-and-block structure of martensite.

A weak effect of deformation on the crystal geometry of the structure of martensite is confirmed by the spectra of the off-orientations given in Fig. 9. It can be seen that the deformation of the initial austenite influences inconsiderably both the low-angle/large-angle proportion of the components of the spectra and the form of these components. This result does not match fully the expected contribution of the strain-induced structure inherited from the austenite into the

⁶ Note that the angles of interblock off-orientations have been computed for a specific orientation relation and can differ somewhat from experimental angles. For example, the maximum in Fig. 6b corresponding to boundaries $V1/V4$ is displaced by 6° with respect to the computed value of 5.4° .

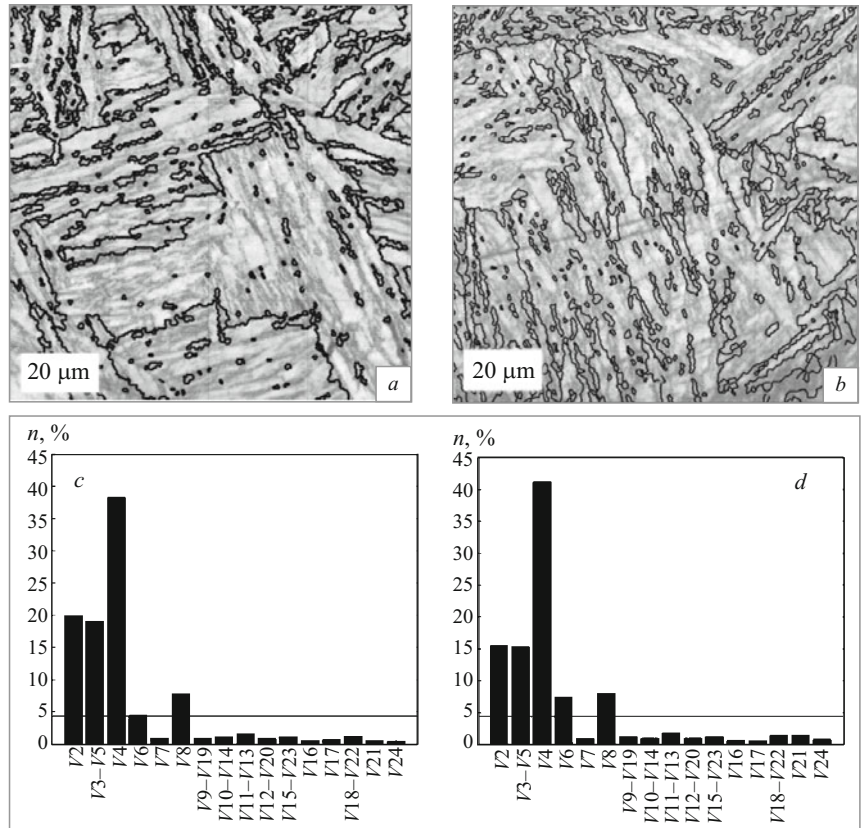


Fig. 8. Structure of steel 2 with $d_v = 160 \mu\text{m}$ represented as a map of distribution of the parameter of the quality of EBSD-image IQ with superimposed contours of the boundaries (the black lines) with off-orientations exceeding 40° (*a, b*) and relative lengths of the CSB (*c, d*): *a, c*) after cooling without deformation in the austenitic range; *b, d*) after deformation with strain $\varepsilon = 50\%$.

low-angle maximum. This may be explained by the fact that the low-angle off-orientations between the strain bands of subgrains in the austenite [13] are random with respect to the off-orientations on the CSB in the transformed structure. In the distribution of the off-orientations of the transformed structure this may cause only little perturbation of the low-angle part without affecting the large-angle regions. As for the transverse boundaries of the subgrains of the austenite, they are chiefly characterized by too low angles $\theta < 2^\circ$, which are worse detectable by the EBSD-methods and therefore are not allowed for in the present work.

CONCLUSIONS

1. In low-carbon low-alloy steels the degree of fragmentation of the austenite due to hot deformation is relatively low, and the level of the off-orientations decreases substantially upon growth of the size of the austenite grains. Characteristic features of the deformed state are considerable intragrain gradients of off-orientation at the scale of a grain.

2. The parameters of the packet-and-block structure of bainite in low-carbon alloy steels depend substantially on the cooling mode. Growth in the cooling rate decreases the size of effective grains by more than a factor of 2. The structure is refined due to the marked change in the kind of the “choice of variants,” i.e., the frequency and mutual arrangement of crystallites having different lattice orientations. Comparison

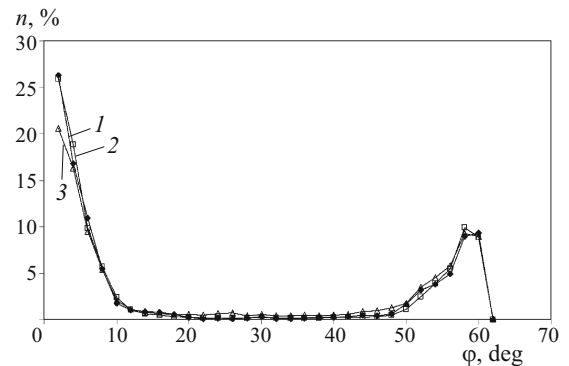


Fig. 9. Distribution of off-orientations in steel 2 with $d_v = 80 \mu\text{m}$: 1) after cooling without deformation in the austenitic range; 2, 3) after deformation with strain $\varepsilon = 30$ and 50% respectively.

of these results with published data allows us to assume that the choice of variants in bainite depends on the temperature range in which the bainite structure forms under continuous cooling. In addition to the growth in the number of places of nucleation of α -phase this factor is responsible for the effect of the deformation of the austenite.

3. In contrast to bainite, the size and crystal geometry parameters of the packet-and-block structure of the martensite depend little on the structural state of the initial austenite, which limits the possibilities of control of the size of effective grains in martensitic steels.

4. Maximum refinement of the final structure of low-carbon alloy steels subjected to deformation in the austenitic temperature range is attained upon formation of lath bainite in them from fine-grained austenite in the middle or bottom part of the temperature range of the bainitic transformation.

REFERENCES

1. Yu. G. Andreev, L. N. Devchenko, E. V. Shelekhov, and M. A. Shtremel, "Packing of martensite crystals in a pseudo-monocrystal," *Dokl. Akad. Nauk SSSR*, **237**(3), 574 – 576 (1977).
2. V. M. Schastlivtsev, L. B. Blind, D. P. Rodionov, and N. L. Yakovlev, "Structure of a martensite packet in structural steels," *Fiz. Met. Metalloved.*, **66**, 759 – 769 (1988).
3. A. Lambert-Perlade, A. F. Gourgues, and A. Pineau, "Austenite to bainite phase transformation in the heat-affected zone of a high strength low alloy steel," *Acta Mater.*, **52**, 2337 – 2348 (2004).
4. S. Morito, X. Huang, T. Furuhashi, T. Maki, and N. Hansen, "The morphology and crystallography of lath martensite in alloy steels," *Acta Mater.*, **54**, 5323 – 5331 (2006).
5. N. Takayama, G. Miyamoto, and T. Furuhashi, "Effects of transformation temperature on variant pairing of bainitic ferrite in low carbon steel," *Acta Mater.*, **60**, 2387 – 2396 (2012).
6. A. Lambert-Perlade, A. F. Gourgues, J. Besson, et al., "Mechanisms and modeling of cleavage fracture in simulated heat-affected zone microstructures of a high-strength low alloy steel," *Metall. Mater. Trans. A*, **35A**, 1039 – 1053 (2004).
7. Z. Guo, C. S. Lee, and J. W. Morris Jr., "On coherent transformations in steel," *Acta Mater.*, **52**, 5511 – 5518 (2004).
8. G. Miyamoto, N. Iwata, N. Takayama, and T. Furuhashi, "Mapping the parent austenite orientation reconstructed from the orientation of martensite by EBSD and its application to ausformed martensite," *Acta Mater.*, **58**, 6393 – 6403 (2010).
9. G. Miyamoto, N. Iwata, N. Takayama, and T. Furuhashi, "Quantitative analysis of variant selection in ausformed lath martensite," *Acta Mater.*, **60**, 1139 – 1148 (2012).
10. G. Iwata, N. Miyamoto, N. Takayama, and T. Furuhashi, "Reconstruction of parent austenite grain structure based on crystal orientation map of bainite with and without ausforming," *ISIJ Int.*, **51**, 1174 – 1178 (2011).
11. A. G. Kozlova and L. M. Utevskii, "Inheritance by martensite of sub-boundaries existing in the austenite of structural steels," *Fiz. Met. Metalloved.*, **37**, 218 – 220 (1974).
12. V. V. Rybin, E. I. Khlusova, E. V. Nesterov, and M. S. Mikhailov, "Formation of structure and properties in low-alloy low-carbon steel due to thermomechanical treatment with accelerated cooling," *Vopr. Materialoved.*, No. 4(52), 329 – 340 (2007).
13. A. S. Taylor, P. Cizek, and P. D. Hodgson, "Comparison of 304 stainless steel and Ni – 30 wt.% Fe as potential model alloys to study the behaviour of austenite during thermomechanical processing," *Acta Mater.*, **59**, 5832 – 5844 (2011).
14. A. S. Taylor, P. Cizek, and P. D. Hodgson, "Orientation dependence of the substructure characteristics in a Ni – 30Fe austenitic model alloy deformed in hot plane strain compression," *Acta Mater.*, **60**, 1548 – 1569 (2012).
15. T. V. Soshina, A. A. Zisman, and E. I. Khlusova, "Determination of former austenite grains by the method of chemical etching in vacuum in imitation of TMT of low-carbon steel," *Metallurg*, No. 2, 63 – 70 (2013).
16. N. Yu. Zolotarevskiy, E. V. Nesterova, A. S. Rubtsov, and V. V. Rybin, "Large-angle boundaries appearing in phase transformations," *Poverkhnost'*, No. 5, 30 – 35 (1982).
17. V. V. Rybin, *High Plastic Strains and Ductile Fracture* [in Russian], Metallurgiya, Moscow (1986), 224 p.
18. S. M. van Bohemen, M. J. Santofimia, and J. Sietsma, "Experimental evidence for bainite formation below M_s in Fe – 0.66C," *Scr. Mater.*, **58**, 488 (2008).
19. E. V. Nesterova, N. Yu. Zolotarevskiy, Yu. F. Titovets, and E. I. Khlusova, "Inheritance of off-orientations and model of formation of bainite structure in low-carbon steels under the effect of deformation of the austenite," *Vopr. Materialoved.*, No. 4(68), 17 – 26 (2011).